Chapter 8
Air Flow Sensing in Bats

Susanne J. Sterbing-D'Angelo and Cynthia F. Moss

Abstract Bats are the only mammals capable of powered flight, and impress with complicated aerial maneuvers like tight turns, hovering, or perching upside-down. The bat wing membrane is covered with microscopically small hairs that are associated with a variety of tactile receptors at the follicle. The directionality profile of neuronal responses to air flow—as measured in the somatosensory cortex of the bats—indicates that the hairs respond strongest to reverse airflow, and might therefore act as stall detectors. We found that depilation of different functional regions of the wing membrane alters flight behavior in obstacle avoidance tasks by reducing aerial maneuverability, as indicated by wider turning angles and increased flight speed. We provide here for the first time electrophysiological and behavioral data showing that bat wing hairs are involved in sensorimotor flight control by providing aerodynamic feedback.

Abbreviations

CX	Cerebral cortex
D	Digit
IC	Inferior colliculus
IFM	Interfemoral membrane
K20	Monoclonal keratin antibody
OB	Olfactory bulb
S1	Primary somatosensory cortex
SC	Superior colliculus

S. J. Sterbing-D'Angelo (✉)
Institute for Systems Research, University of Maryland, Building 144,
College Park, MD 20742, USA
e-mail: ssterbin@umd.edu

C. F. Moss
Department of Psychology, Institute for Systems Research, University of Maryland,
Building 144, College Park, MD 20742, USA
e-mail: cmoss@psyc.umd.edu

H. Bleckmann et al. (eds.), *Flow Sensing in Air and Water*,
DOI: 10.1007/978-3-642-41446-6_8,

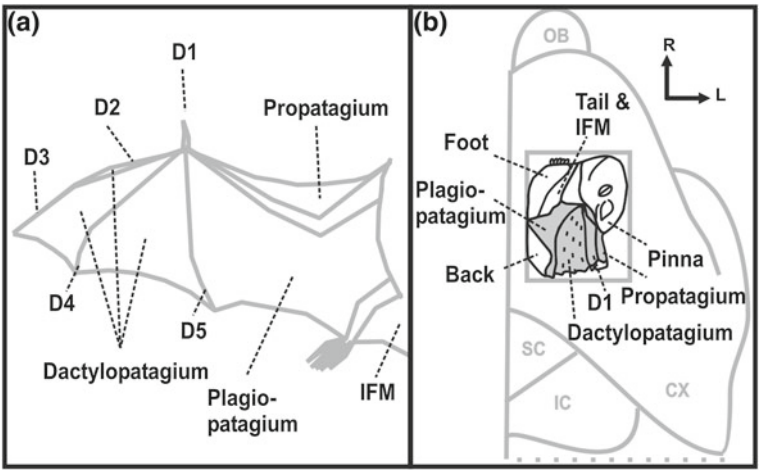

Fig. 8.1 **a** Nomenclature for parts of the bat wing. *D*1–*D*5 digits (1: thumb), *IFM* interfemoral membrane, **b** Schematic brain surface view of the right hemisphere of the Big Brown Bat, *Eptesicus fuscus CX* cerebral cortex, *IC* inferior colliculus, *OB* olfactory bulb, *SC* superior colliculus, *R* rostral, *L* lateral. The *rectangle* indicates the approximate location of the primary somatosensory cortex, S1. The inserted sketch depicts the body representation mapped onto the brain surface. The *wing* representation is marked in *grey*. Note that the *wing* representation covers approximately 1/3 of the entire S1 area surface (see also Sterbing-D'Angelo et al. 2011; Chadha et al. 2010)

8.1 Introduction

Bat flight—the only true, powered flight found in mammals—is characterized by remarkable aerial maneuvers like steep banking, hovering, and landing upside-down. Skeletal specializations (see Fig. 8.1a), muscular control of wing shape, e.g., camber, and the highly compliant characteristics of the wing membrane are the basis of maneuverability and energy efficiency (Swartz et al. 1996; Winter et al. 1998; Voigt and Winter 1999; Stockwell 2001). Moreover, bat flight is very robust in turbulent, gusty, and low Reynolds number air flow conditions, for example during low-speed flight and hovering. While earlier studies relied on high-speed video tracking and modeling to characterize flight (Rayner 1979a, b), recent particle image velocimetry (PIV) experiments showed that these animals produce complex aerodynamic wake patterns (Hedenström et al. 2007; Muijres et al. 2008). However, the sensory-motor mechanisms that underlie the robustness of bats' flight have not been studied in detail, and despite the fact that the wing is well represented in the primary somatosensory cortex (Fig. 8.1b) of echolocating bats (Big Brown Bat—*Eptesicus fuscus* (*E.f.*): Chadha et al. 2010, Pallid Bat—*Anthrozous pallidus* (*A.p.*): Zook and Fowler 1986; Ghost Bat—*Macroderma gigas* (*M.g.*): Wise et al. 1986), we know only little about the nature and function of the cutaneous tactile receptors located in the wing membrane. To the naked eye, the bat's wing membrane appears hairless, in contrast to the head and body of the

animals, which are densely covered with fur. At first thought this appears odd, because fur surfaces are known to stabilize (microlaminarize) the boundary layer airflow by breaking up large vortices into microturbulences (Nachtigall 1979). However, a sparse grid of microscopically small hairs, many of which are protruding from domed structures, is found on both dorsal and ventral surfaces of the bat wing. These hairs were described first in the early twentieth century (Maxim 1912), but their role for bat flight has never been studied until recently (Sterbing-D'Angelo et al. 2011; Zook and Fowler 1986).

Bats typically have a layer of soft vellus hair (undercoat) overlaid with a layer of guard hair that is straighter and coarser. Except for sensory whiskers, bat pelage hair structure is quite uniform over the entire head and body. Big Brown Bat hair, like most microchiropteran bat species pelage (Debelica and Thies 2009), has a spiny coronal scale pattern, i.e., one scale forms a "ring-like" structure. This is only possible because bat pelage hair is amongst the finest of all mammalian hair with a diameter of only 10–20 μm. The main functions of pelage hair is heat insulation, and possibly improving aerodynamics by forming ripplets that reduce parasitic drag associated with skin friction and airflow separation (Bullen and McKenzie 2008). Parasitic drag is maximized or minimized depending upon the extent of turbulence in the boundary layer of air in immediate proximity to the body. In contrast to the pelage found on head and body of bats, the hairs on the wing membrane are too sparsely distributed and too short (100–600 μm) to be involved in heat insulation or in physically influencing the airflow over the wing surface. For the same reason a hypothetical function to avoid wetting of the wing membrane that has been described for insect wing hair (Wagner et al. 1996) can be excluded. The possible functional role for the domed wing hairs of bats has been speculated about for quite a while (Welwitsch's bat, *Myotis welwitschii*, Maxim 1912). But only recently researchers have begun to systematically study the properties of the hairs, and the properties of the tactile receptors that surround them (Zook and Fowler 1986; Zook 2006; Sterbing-D'Angelo et al. 2011). The domes from which the bat wing hairs protrude resemble touch domes (Merkel cell neurite complex) in the skin of non-flying mammals, which are rarely associated with hairs (Pinkus 1902; Smith 1977). Preliminary histological studies (Zook and Fowler 1986; Zook 2006) revealed a considerably large population of presumptive Merkel cells concentrated at the basement membrane along the dome surface and surrounding the hair follicle of the Pallid Bat. In congruence with the classic description of Merkel cells (Pinkus 1905; Smith 1977; Halata et al. 1993; Haeberle et al. 2004), these cells were typically large, clear cells with lobulated nuclei restricted to the epidermal basal lamina. Staining of these cells with both Merkel-specific quinacrine fluorescence (Nurse et al. 1983) and a cell-specific antibody to the cytokeratin protein, CK20 (Moll et al. 1995) further confirmed the identification as Merkel cells. Nerve fibers within the dome complex can be traced to individual Merkel cells in *A.p.* and *E.f.* (Zook 2005). Other tactile receptors have been identified in early anatomical studies (e.g., Ackert 1914). Recently, a fluorescent marker study confirmed that free nerve endings and lanceolate receptors are present at the wing hair base of the Big Brown Bat (Chadha et al. 2012). In this

species, it turns out that only a subset of wing hairs stained positive for Merkel cells, while the majority of hair follicles were surrounded by lanceolate endings. Since Merkel cells are known as "slowly-adapting" tactile receptors, and lanceolate endings as "rapidly adapting" receptors (Adrian 1941), it is likely that both receptor populations code for different air flow parameters. The sensory hairs on the bat wing are very stiff, with an average taper of 10 and a transversal elastic modulus of 500 MPa, typical for α-keratin. During deflection, the mechanical impact on the closely surrounding receptor cells, lanceolate endings, as well as Merkel cell neurite complexes, has been modeled to be so substantial at biological flight speeds, providing evidence that the classification of the wing hairs as airflow sensors is warranted. Hence, our hypothesis is that the domed wing hairs provide aerodynamic feedback to the somatosensory brain, and are therefore involved in flight stabilization. Sensilla on the wing and other body parts of insects have been shown to play a role in flight control (e.g., Haskell 1958; Pflueger and Tautz 1982; Dickinson 1990; Ai et al. 2010), as have vibrotactile receptors at the feather base of birds (Necker 1985; Hoerster 1990). Hence, we studied how neurons in the primary somatosensory cortex respond to experimental air flow stimuli, and how the removal of wing hairs influences flight behavior.

8.2 Methods

Detailed methods of the experimental procedures, data acquisition, and analysis have been published elsewhere (Sterbing-D'Angelo et al. 2011; Chadha et al. 2012). Therefore, we only provide a short summary here.

8.2.1 Animals

Eptesicus fuscus (*E.f.*) were wild-caught in Maryland. *Carollia perspicillata* (*C.p.*) and *Glossophaga soricina* (*G.s.*) were donated (Montréal Biodôme, Canada), and bred in a captive colony. All bats were housed under reversed 12 h light/dark conditions with appropriate temperature and humidity levels for each species. *C.p.* and *G.s.* were maintained on a diet of various fruits, nectar, and water. *E.f.* were maintained on a diet of mealworms, *Tenebrio molitor*, and water. All procedures were approved by the University of Maryland Institutional Animal Care and Use Committee.

8.2.2 Scanning Electron Microscopy

Circular wing membrane samples (13 mm dia.) from 24 different locations of 2 *E.f.* (12 each), 8 samples from the wing of each one *C.p.* and *G.s.* at corresponding locations, except tail membrane, were fixed in 2.5 % glutaraldehyde solution,

washed in phosphate buffer, and then fixed in 1 % buffered osmium tetroxide. After standard washing and dehydration procedure, the samples were dried in a critical point dryer (Denton DCP-1), and mounted onto metal pedestals with silver paste, hardened at 50 °C, and then coated with gold palladium alloy (Denton DV-502/502 Vacuum Evaporator). The samples were viewed in a scanning electron microscope (Amray AMR-1610). For immunohistochemistry, bat wing was fixed in 4 % paraformaldehyde, cryoprotected with sucrose, frozen, and sectioned at 20 μm.

8.2.3 Experimental Procedures

For surgery and electrophysiological recordings, *E.f.* were anesthetized with 1–3 % isoflurane mixed with 700 ml/min O_2. Breathing rate was monitored visually, and body temperature was maintained at about 37 °C by placing the animal on a heating pad. Standard sterile surgical procedures were followed throughout the experiment. After exposing the skull, a custom-made stainless steel head-post was glued close to Bregma using cyanoacrylate glue. Bats were allowed to recover for 2–3 days before electrophysiological recordings were initiated. A craniotomy (intact Dura mater) measuring approximately 2 × 2 mm was made to expose the somatosensory cortical region, and sterile saline/silicone oil (Fluka Analytical, DC 200) was used to prevent the exposed brain surface from desiccation. Either a high impedance recording electrode (15–20 MΩ tungsten, FHC Inc.) was used to record extracellularly from multi-neuron clusters or a silicon probe was used (Neuronexus). The electrode/probe entered the cerebral cortex perpendicularly to the surface and was positioned using 3 digital microdrives (Mitutoyo). Recordings were made from multiple electrode penetrations from depths of 50–250 μm, ensuring that the recordings were made mostly within the supragranular layers of the cortex according to a standard brain atlas of *E.f.* (Covey, unpublished). The contralateral wing was spread and secured to the recording table. Tactile receptive fields were measured by using a set of calibrated monofilaments (von Frey hairs, North Coast), applying pressure on a logarithmic scale from 0.008 to 300 g (equals 0.08–2,943 mN), with a 5 % standard deviation. Both wing surfaces were tested. For stimulation with air puffs a syringe was directed at the center of the receptive field from different angles in 45° or 90°. steps. Air puff stimuli were generated by a dispensing workstation (EFD Ultra®2400), and electronically varied in duration and amplitude. Air flow was calibrated (Datametrics 100VT-A). At each recording site, the magnitude of the air puff was adjusted to be just above the neuronal threshold, verified by microscopic inspection that no indentation of the membrane occurred. The workstation trigger also started the data acquisition board that recorded the waveform of the neural responses after amplification (Bak Electronics, Plexon Omniplex). Each stimulus was presented 20 times with an interstimulus interval of 10 s. Single neuron activity could be extracted by standard offline spike sorting (Neuroexplorer v.3,

Offline Sorter v.3, Plexon). At the end of the recording sessions, bats were given a lethal dose (0.05 ml) of sodium pentobarbital (390 mg/ml, i.p.). Data collected under research protocol, "Somatosensory signaling for flight control," approved by the University of Maryland Institutional Animal Care and Use Committee.

8.2.4 Flight Testing

Flight path recordings were conducted in a carpeted flight room (7 × 6 × 2.5 m), with acoustic foam on walls and ceiling (Sonex) under low-intensity, long-wavelength light conditions high-speed (>650 nm, incandescent bulbs filtered through Plexiglas G2711; Atofina Chemicals). Two high speed (250 frames per second) infrared video cameras (FASTCAM-PCI-R2) were used to record 3D position of bat and obstacles. *E.f.* and *C.p.* were trained to perform rewarded obstacle flight tasks (see Fig. 8.7a, b) that required flight maneuvers (details in Sterbing-D'Angelo et al. 2011, and in results section). The flight data were collected before and after depilation of the wing hairs (Veet®). Flight speed and turn angles were calculated from the high-speed videos.

8.3 Results

8.3.1 Hair Morphology and Distribution

The morphology and distribution of wing hairs were examined for three echo locating species, the Big Brown Bat (*Eptesicus fuscus, E.f.*), the Short-Tailed Fruit Bat (*Carollia perspicillata, C.p.*), and Pallas's Long-Tongued Bat (*Glossophaga soricina, G.s.*) using scanning electron microscopy. The ecological niches and diets of these three bat species differ and consequently impact requirements for flight control. In particular, the insectivorous *E.f.* must make sharp turns in flight to pursue and capture evasive insect prey, the frugi-/nectarivorous *C.p.* must maneuver through dense vegetation to find fruit, and the nectarivorous *G.s.* must hover over flowers to take nectar. In all three species, the short hairs are sparsely distributed along dorsal and ventral surfaces of the wing, and are morphologically distinct from the long pelage hairs. The pelage hairs were only found on SEM samples that were cut close to the limbs. They were up to several milimeters long, relatively thick at the base (6–18 μm) found close to the ventral forearm, around the leg, and on the tail membrane, sometimes referred to as inter-femoral membrane (IFM) or uropatagium (Fig. 8.1).

In all three species, on the membraneous parts of the wing, a second type of hair was found, which is invisible to the naked eye. These hairs are so thin that only one follicle cell builds each segment of the hair, resulting in a coronal scale

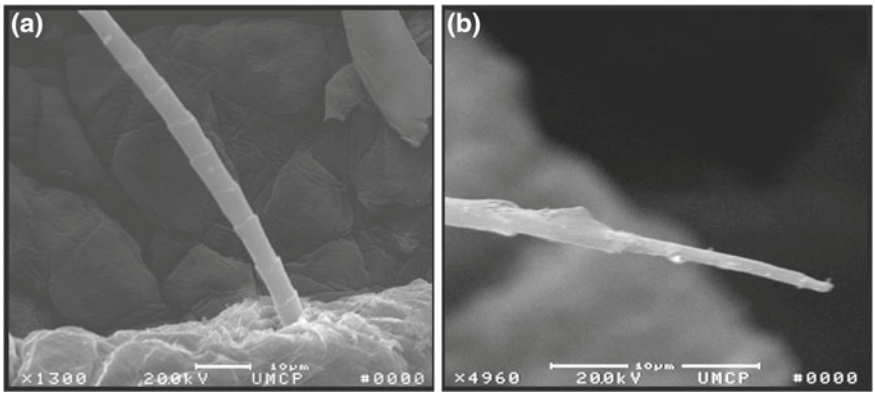

Fig. 8.2 Scanning electron microscope images of hairs from the wing membrane of the Big Brown Bat, *Eptesicus fuscus*. **a** Base of a hair (diameter ~5 µm) protruding from a dome-like structure. Note the coronal scale pattern. **b** Tip of a hair (diameter ~400 nm). The calibration bars located on the bottom of both images indicate 10 µm

pattern. The tip diameter of these hairs is only 200–900 nm, if they are intact (Fig. 8.2). These small hairs are typically found in rows, generating a sparse grid of about one hair per mm^2. This finding confirms early studies, e.g., (Ackert 1914), who described that "the proximal parts of the membranes are covered with fine hairs similar of those of the pelage, while over the distal areas extremely fine, more or less *modified* hairs occur sparsely."

In the two phyllostomid species, *C.p.* and *G.s.*, the distribution of the hairs, as well as their length and thickness, are similar to *E.f.* except that in some areas of their wing membrane, particularly on the dorsal plagiopatagium at the trailing edge and on the propatagium (part of the leading edge of the wing), several hairs—typically three to five-protrude from one dome in clusters (Fig. 8.3a, b), a finding that has been previously described for *A.p.* (Zook 2006). In *E.f.*, only very rarely two hairs can be found right next to each other (Fig. 1.4). Theoretical considerations and modeling of boundary layer detection reveals that the measured hair lengths shown here are in very good agreement with the theoretical ideal length of hair for maximum shear-force sensitivity to boundary layer shape and avoidance of viscous coupling, may be with the exception of hairs within a multi-hair cluster (Dickinson 2010).

8.3.2 Tactile Receptors in the Wing Membrane

A variety of receptors have been found in the bat wing membrane. Figure 8.4 shows rings of fluorescent-marked Merkel cells around wing hairs in *E.f.*, stained with topically applied Rhodamine. Furthermore, preliminary data of our collaborators at Columbia University (E. A. Lumpkin and K. L. Marshall; see Chadha et al. 2012) revealed that many hairs are co-localized with lanceolate nerve

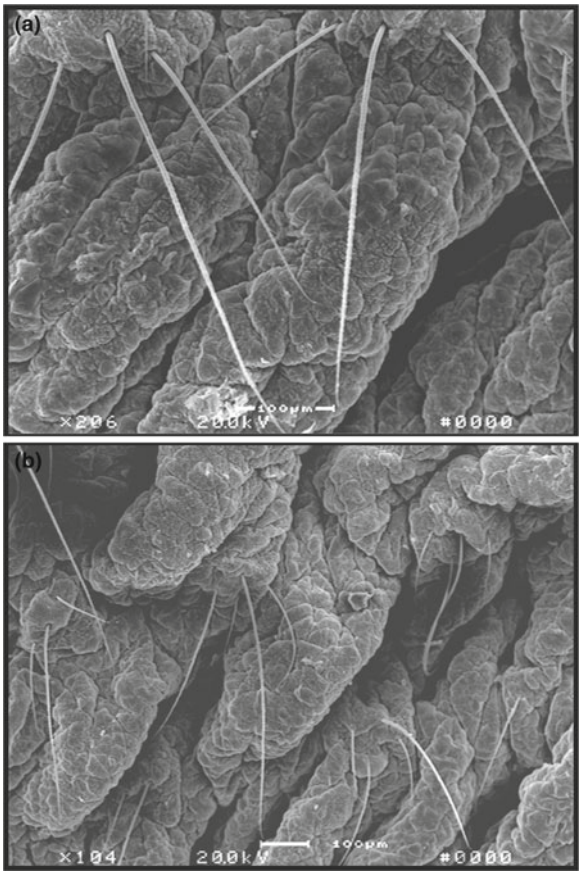

Fig. 8.3 **a** Scanning electron microscope image of hairs from the wing membrane of the Short-Tailed Fruit Bat, *Carollia perspicillata*. This sample was taken from the dorsal plagiopatagium close to the trailing edge. Three to five hairs protrude from each domed structure (calibration *bar*: 100 μm); **b** Image of hairs from the same region on the wing membrane of the Pallas's Long-Tongued Bat, *Glossophaga soricina*. Note that the membrane of this extracted sample is folded up due to embedded elastin bands. During flight, the membrane would be stretched out flat

endings, a finding that confirms an earlier report for a different bat species (Ackert 1914). For a subset of wing hairs, the K20 antibody additionally marked Merkel cells (Chadha et al. 2012) confirming preliminary data by Zook (2005). Free nerve endings and other endings marked by Peripherin were found throughout the epidermis (Chadha et al. 2012).

8.3.3 Cortical Neuronal Responses to Air Flow: Directionality

Single neuron as well as multi-neuron cluster responses in the primary somatosensory cortex of the big brown bat varied with spatially restricted (diameter of stimulated wing area <8 mm) air flow from different direction (Sterbing-D'Angelo et al. 2011; Chadha et al. 2012). Air puffs were delivered to the dorsal wing surface from eight directions in 45° steps for the multi-units and from the four major

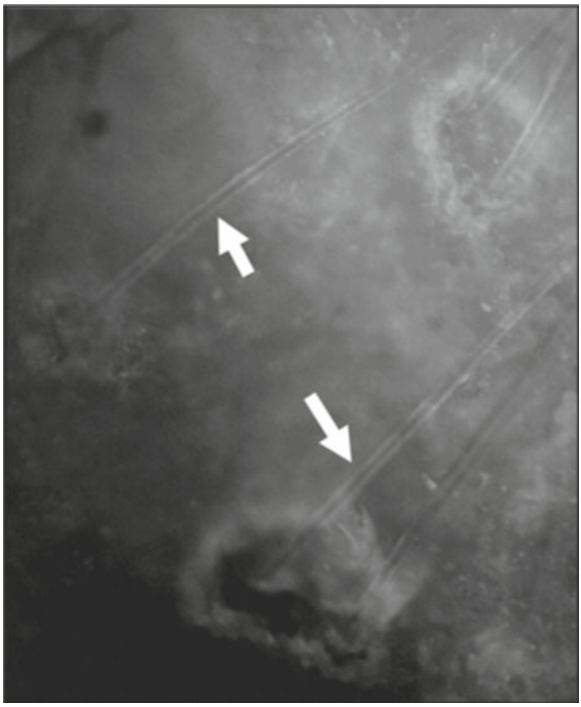

Fig. 8.4 Microphotograph of Rhodamine-stained fluorescent Merkel cells in a whole wing mount of an isoflurane-anesthetized Big Brown Bat, *Eptesicus fuscus* Merkel cells form a well-organized partial or full circle around the hair follicle. *Arrows* point to some of the hairs that emerge from the ring-like structures

directions for the single units. The multi-unit responses were half-wave rectified and averaged across the 20 trials. The responses for each stimulation direction were normalized to maximum, and plotted as polar diagrams. Minimum–maximum ratio between the best (preferred) and worst direction was calculated to quantify the strength of directionality of the air puff response of 20 multi-units from 4 *E.f.* Most units, 9/9 single units and 15/20 multi-units—although their receptive fields were located on different areas of the dorsal wing membrane—favored air flow from the rear (135–225°). The only exceptions were multi-units with receptive fields located on the extreme leading edge of the wing, and those with receptive fields close to the body. The responses of the latter might have been influenced by turbulences caused by the proximity of elevated body features. Figure 8.5a shows polar plots of normalized multi-neuron responses to air flow from different directions.

8.3.4 Cortical Neuronal Responses to Air Flow: Temporal and Spatial Characteristics

Recordings with silicon probes (Neuronexus) collected responses from various sites on the wing membrane simultaneously. The multi-neuron responses at each probe were sorted to extract single neuron activity. Figure 8.5b shows responses of single neurons to 40 ms air puffs (stimulated wing area $\sim$8 mm in diameter)

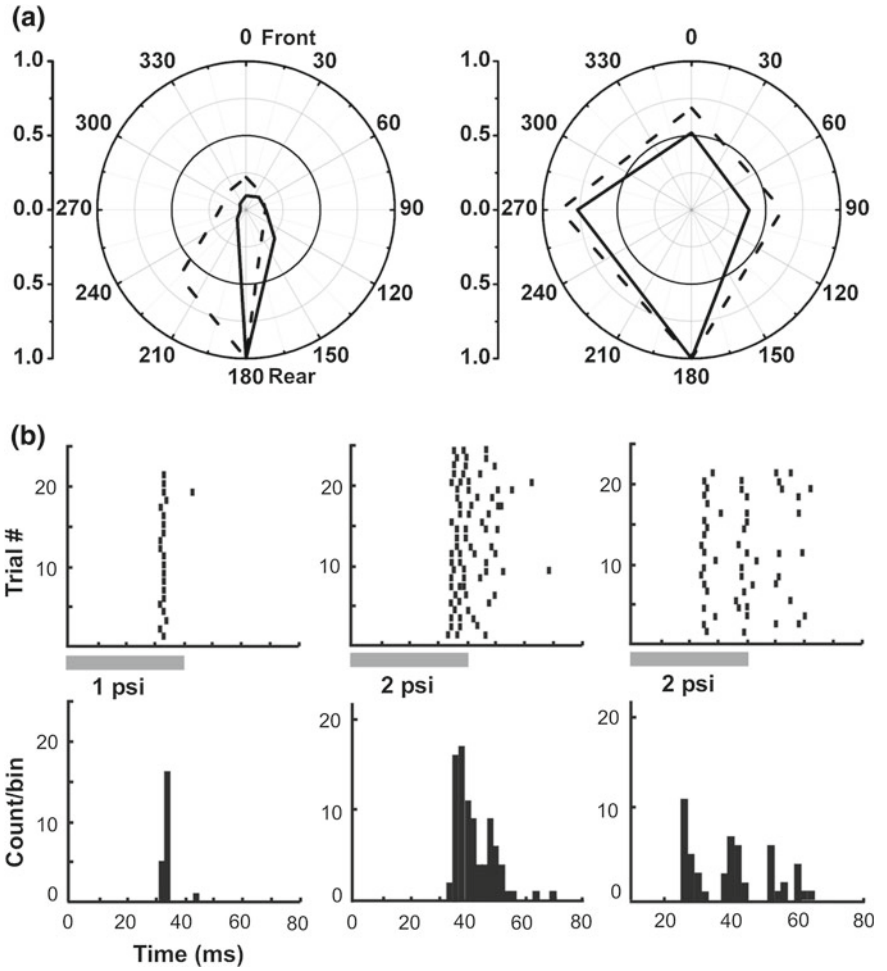

Fig. 8.5 **a** Polar plots depicting the directionality of *wing* hair responses in primary somatorensory cortex of *Eptesicus fuscus* Units could show sharp (*left*) or wider tuning (*right*) to pseudo-randomly chosen directional air flow. The *hatched lines* indicates results from a repeated set of stimulations minutes after the initial data set (*solid lines*) was recorded, showing that the directionality of the units was well preserved over time. **b** Spike raster plots of a phasic, a sustained, and a complex firing single neuron, recorded from primary somatosensory cortex of *Eptesicus fuscus* (Chadha et al. 2012)

presented from the neuron's preferred direction at different airflow velocities. The single neuron responses were phasic, sustained, or "complex" with periodic spike patterns that could indicate a preference for deflection close to the resonance frequency of the hairs, an effect that has been described for a whisker model (Williams and Kramer 2010).

When a receptive field was identified on the wing membrane, two blunt syringe needles were positioned so that their openings pointed to the same location on receptive field center, one from the dorsal and one from the ventral side, at a fixed measured distance (for most units 3 mm) from the wing surface. An air flow magnitude that just elicited a weak response, and therefore was close to threshold was chosen and delivered first to either side of the membrane alone, and then to both sides simultaneously. For most units (7/9 recorded from two animals) we found evidence for facilitation when both surfaces were stimulated simultaneously, which means that the unit's response was stronger than the sum of the responses to stimulation of either side alone. Figure 8.6 shows examples of facilitation in S1 recordings collected from two bats. The facilitation effect appears to be strongest close to threshold of the respective neuronal cluster. At high supra-threshold air stimulation levels, it cannot be ruled out that cutaneous receptors other than the receptors at the hair base are contributing to the response, because the entire wing membrane is increasingly indented with stimulus intensity, in addition to the deflection of the hairs.

8.3.5 Flight Behavior

The schematics in Fig. 8.7a, b illustrate the setups used to study the role of wing hairs in flight control for obstacle avoidance in two bat species, *E.f.* and *C.p.*. Several *E.f.* were trained to fly through an artificial forest (Fig. 8.7a) and *C.p.* were trained to fly though openings in a series of nets which created a maze (Fig. 8.7b). The artificial trees were nearly cylindrical, constructed out of visually transparent nets, to allow us to continuously monitor the bat's flight path with video cameras. Both species gained access to a food reward for successfully maneuvering around obstacles. Flight behavior was monitored with two high-speed video cameras mounted in corners of the room. With the stereo video recordings, we are able to reconstruct the 3-D flight paths of the bats as they performed the tasks. In all of the behavioral experiments, bats were run under baseline, and experimental conditions. Baseline recordings were conducted over a minimum of twenty trials, to establish the norms of the bat's flight behavior. Then, the experimental trials were conducted, in which hairs are removed from selected regions of the wings, using a depilatory cream (Veet®). Absence of hairs was confirmed by microscopic inspection.

Removing the tactile wing hairs of the trailing edge resulted in higher average flight speed and reduced angular turn angle (i.e., wider turns) as the treated bat approached an obstacle, compared to baseline. Although comparing bat flight to fixed-wing aircraft flight is problematic, increasing air speed is also recommended to pilots to recover from stalls. We interpret the depilated bats' increase average flight speed as a result of lacking input from the domed hair receptors to the somatosensory system. Our findings that neural responses to airflow are directional suggest that wing sensors may play a role in stall detection. In the behavioral task,

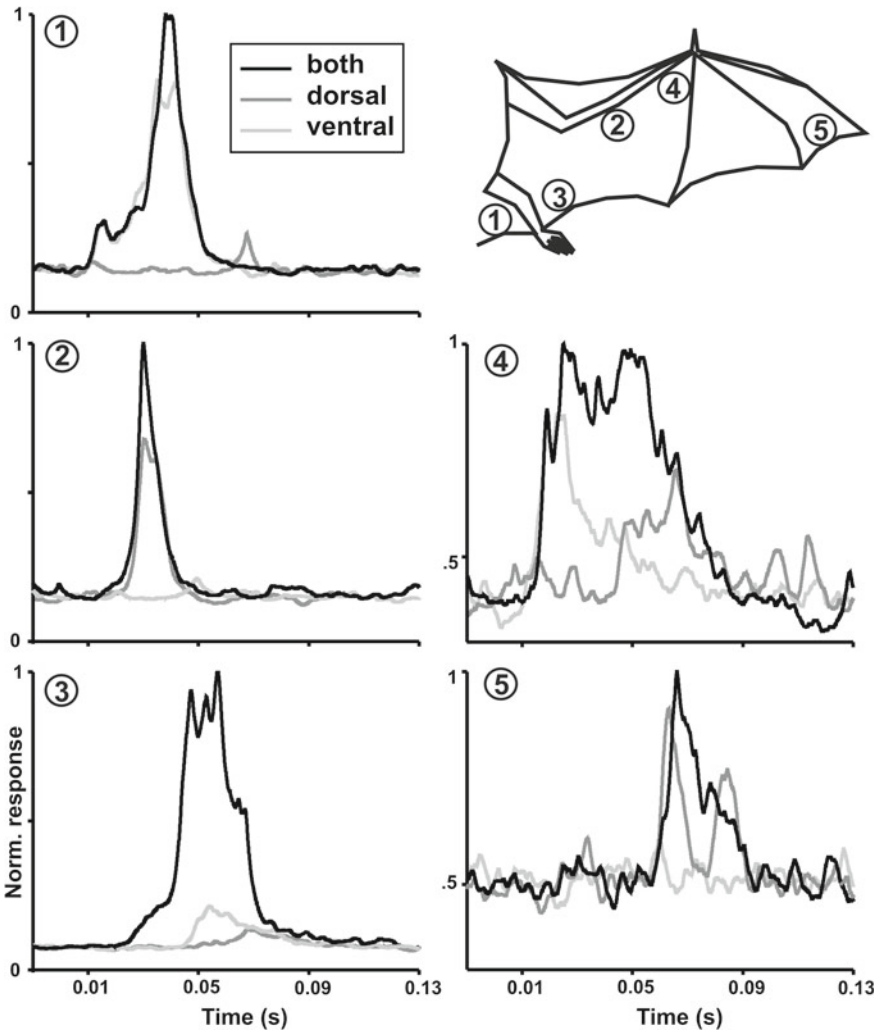

Fig. 8.6 Somatosensory (S1) responses of five multi-neuron clusters with receptive fields located on different *wing* areas at near-threshold stimulation with air puffs of 40 ms duration. The lines indicate averages of 20 trials for each condition (*both*, *dorsal* only, *ventral* only). In case of stimulation of both surfaces, the air flow was split with valves to ensure that the total air mass reaching the *wing* membrane was kept constant. Two syringes were directed at the center of the receptive field at the same distance and angle from both the *dorsal* and *ventral* side of the membrane. Air puffs stimulated either the *dorsal* surface of the wing alone (*medium gray*), the *ventral* surface of the *wing* alone (*light gray*), or both the *dorsal* and *ventral* surfaces of the wing simultaneously (*black*). For most units, responses were facilitated by simultaneous stimulation of *both* surfaces, although the air mass reaching each surface was split in half to keep the overall air mass that reaches the membrane constant

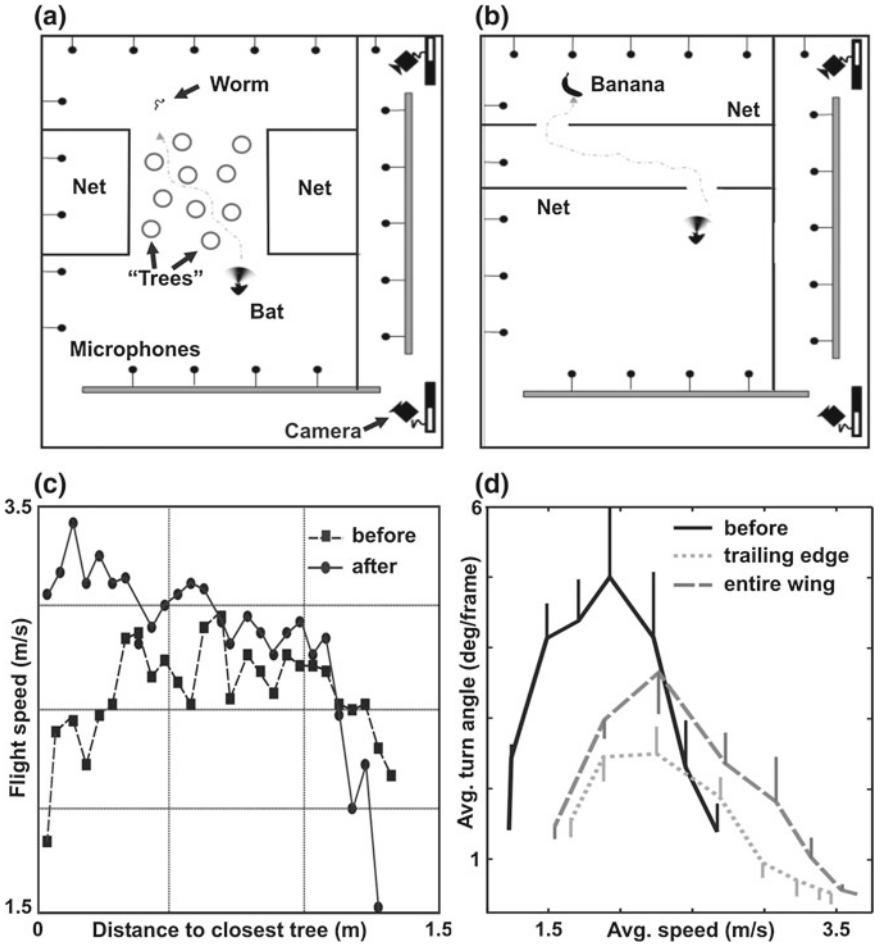

Fig. 8.7 **a, b** Schematic of setups to record flight behavior of *Eptesicus fuscus* through an artificial forest (**a**), and of *Carollia perspicillata* through a net maze (**b**). Both tasks required turning in flight to avoid obstacles. In both setups, two high-speed video cameras recorded flight behavior, and 3-D flight paths were reconstructed. **c** Flight speed versus distance to the closest tree is plotted for one *Eptesicus fuscus*, before and after depilation (mean of 10 trials from one animal). Note that the overall flight speed increased. **d** Flight speed versus average turn angle for *Carollia perspicillata,* before depilation, and after depilation of the hairs along the trailing edge only, and later the entire wing (2 animals, 117 trials, mean ± SE). Also in this species, and for this task, flight speed and average turn angle changed after depilation. However, the depilation of the trailing edge only seems to have a greater effect than the depilation of the entire wing surface

a depilated animal may fly faster and make wider turns compared to baseline in an attempt to avoid a stall by speeding up, because reverse airflow signals have been disrupted, and the treated animal may have experienced that it is more vulnerable to stall. Alternatively, the hairs may simply function as flight velocity sensors, and the depilated bat would interpret a lack of input from the hairs as low-speed, and

consequently change its flight speed. Of course, also kinesthetic and proprioceptive inputs are still available to the bat, and it remains an open question the extent to which a bat can adapt to the absence of wing hairs over time. We tested the flight performance within two days of depilation. It is unclear if, and in which time frame, the domed hairs grow back.

8.4 Discussion

The sparse distribution of sensory hairs on the bat flight membrane, as well as their small size, has eluded formal demonstration of their function for decades; however, these very anatomical features provide compelling evidence for their role in air flow sensing for flight control. At the microscopic scale viscous force is dominant, and viscous coupling occurs especially at the low Reynolds numbers (*Re*) (down to only $Re = 5{,}000$ for hovering flight), typically observed in bat flight. Viscous coupling can be observed over a distance of 50 hair diameters or even more (Casas et al. 2010; Heys et al. 2008; Cummins et al. 2007). Coupling leads to sensory "dead zones" between hairs, and a more dense distribution of hairs on the membrane would not only add weight, but also increase highly nonlinear ensemble reactions to air flow that might "blur" the information carried by the tactile input. Hence, a sparse distribution of air flow sensing hairs seems to be advantageous in many respects. Interestingly, the diameter, length and average distance of hairs in the bats of our study are quite similar to those found for filiform hairs on the cerci of crickets (diameter: 1–9 μm, length: 30–1,500 μm, Shimozawa and Kanou 1984), but less variable. The cercal filiform hairs sense velocity, acceleration, and direction of air flow. Measurement of viscous coupling between these filiform hairs revealed that hairs might influence each other up to a distance of about 400 μm. Arthropod filiform hairs, however, have much lower thresholds for air flow velocity (0.03 mm/s) than the bat wing hairs (20–30 mm/s, under isoflurane anesthesia), obviously due to the fundamentally different sensory receptor properties between mammals and arthropods, but also as adaptation to physiological flight speeds (upto 8–10 m/s). At a given distance, viscous coupling is stronger for hairs of similar length than different length. We found that the length of the tactile hairs systematically varied along the rostro-caudal axis with the longest ones located close to the proximal forelimb (300–600 μm) and the shortest close to the trailing edge of the wing (100–300 μm). In some bat species, apart from *E.f.*, groups of sensory hairs protruding from a single dome were reported (*A.p.*: Zook 2006, *C.p.* and *G.s.*: our study). The hairs within the "tufts" tend to have very different lengths, possibly to minimize viscous coupling effects. The sharp taper of the hairs on the wing membrane, in comparison to pelage hairs, is very similar to the taper of whisker (sinus) hairs of rodents (~ 10), although the wing hairs are morphologically not sinus hairs, and of much smaller scale than whiskers. The taper reduces the maximum deflection angle of the entire hair, which leads to higher spatial acuity than estimates for more bluntly tapered hairs

(Williams and Kramer 2010). Since periodic spiking was frequently observed in our single neuron responses recorded in S1, a sharp taper would also improve the robustness for changes in resonance frequency, which would keep periodicity coding in the somatosensory cortex in a stable range. Preliminary laser scanning vibrometer tests performed on hairs from the Big Brown Bat revealed natural frequencies between 60 and 80 Hz. Hence, the role of the sensors at the base of the hairs might serve different purposes. Firstly, they could provide sensory feedback for lift control by sensing the size and location of the leading edge vortex. The importance of the leading edge vortex for generating additional lift has been pointed out by (Muijres et al. 2008). Secondly, by detecting reverse air flow that compromises flight stability, signals from the hairs could be used to prevent stall. Finally, the rapidly adapting receptors, in particular, would provide information of sudden changes in air flow direction. Thus, we propose that the rapid-adapting and the slow-adapting receptors at the hair base have different functional roles: the fast-adapting lanceolate endings are well suited for detecting sudden changes of airflow conditions, e.g., during wind gusts or turbulence. In contrast, the slow-adapting receptors like Merkel cells are better suited to detect overall air flow patterns across the wing, and monitor the dimension of the leading edge vortex. Of course, Merkel cells and lanceolate cells are not the only receptor types that potentially could influence flight performance: stretch receptors, especially those in the plagiopatal muscles most likely influence the shape of the wing membrane, and possibly also signal local membrane oscillations caused by turbulences (Swartz et al. 2005). In our depilation experiments, the resulting changes in flight maneuverability were measurable but not dramatic, at least for the geometric setups that were used. One reason is that the bats still have the information from all types of tactile receptors that are embedded in the skin, and which are unaffected by the depilatory cream. Besides nerve endings on hairs, Ackert (1914) and others described free nerve endings, special sensory end organs like "end bulbs," "terminal corpuscles," motor nerve endings on striated muscles, and nerve endings on modified sweat glands in the wing membrane of bats. The removal of the hairs which act as levers merely causes a reduction of the most effective way to stimulate the receptors at the hair base. Also, general kinesthetic information is still available to the bat after depilation. It is known that bats become familiar with the environment very quickly, and that they may also orient using kinesthetic memory. Further investigation will be aimed at the different contributions to flight behavior of the individual receptor types.

Acknowledgments This study was sponsored by air force office of scientific research (AFOSR), MURI grant "Bio-inspired flight for micro-air vehicles." Data collected under research protocol, "Somatosensory signaling for flight control," approved by the University of Maryland Institutional Animal Care and Use Committee. We thank Mohit Chadha, Wei Xian, Ben Falk, and Aaron Reynolds for contributions.

References

Ackert JE (1914) The innervations of the integument of chiroptera. J Morphol 25:301–334
Adrian ED (1941) Afferent discharges to the cerebral cortex from peripheral sense organs. J Physiol 100:159–191
Ai H, Yoshida A, Yokohari F (2010) Vibration receptive sensilla on the wing margins of the silkworm moth *Bombyx mori*. J Insect Physiol 56:236–246
Bullen RD, McKenzie NL (2008) Aerodynamic cleanliness in bats. Austral J Zool 56:281–296
Casas J, Steinmann T, Krijnen G (2010) Why do insects have such a high density of flow-sensing hairs? Insights from the hydromechanics of biomimetic MEMS sensors. J R Soc Interface 7:1487–1495
Chadha M, Moss CF, Sterbing-D'Angelo SJ (2010) Organization of the primary somatosensory cortex and wing representation in the Big Brown Bat, *Eptesicus fuscus*. J Comp Physiol A 197:89–96
Chadha M, Marshall KL, Sterbing-D'Angelo SJ, Lumpkin EA, Moss CF (2012) Tactile sensing along the wing of the echolocating bat. Eptesicus fuscus. Soc Neurosci Abstr 523:03
Cummins B, Gedeon T, Klapper I, Cortez R (2007) Interaction between arthropod filiform hairs in a fluid environment. J Theor Biol 247:266–280
Debelica A, Thies ML (2009) Atlas and key to the hair of terrestrial texas mammals. In: Robert J Baker (ed) Special publications of the Museum of Texas Tech University, vol 55. Museum of Texas Tech University, Lubbock, USA
Dickinson MH (1990) Comparison of encoding properties of campaniform sensilla on the fly wing. J Exp Biol 151:245–261
Dickinson BT (2010) Hair receptor sensitivity to changes in laminar boundary layer shape. Bioinspir Biomim 5:1–11
Haeberle H, Fujiwara M, Chuang J et al (2004) Molecular profiling reveals synaptic release machinery in merkel cells. Proc Natl Acad Sci 101:14503–14508
Halata Z (1993) Sensory innervation of the hairy skin (light-and electronmicroscopic study). J Invest Dermatol 101:75S–81S
Haskell PT (1958) Physiology of some wind-sensitive receptors of the desert locust (*Schistocerca gregaria*). XVth Int Zool Congr, London
Hedenström A, Johansson LC, Wolf M, von Busse R, Winter Y, Spedding GR (2007) Bat flight generates complex aerodynamic tracks. Science 316:894–897
Heys J, Gedeon T, Knott B, Kim Y (2008) Modeling arthropod filiform hair motion using the penalty immersed boundary method. J Biomech 41:977–984
Hoerster W (1990) Histological and electrophysiological investigations on the vibration-sensitive receptors (Herbst corpuscles) in the wing of the pigeon (*Columba livia*). J Comp Physiol A 166:663–673
Maxim H (1912) The sixth sense of the bat. Sir Hiram's contention. The possible prevention of sea collisions. Sci Am 27:80–81
Moll I, Kuhn C, Moll R (1995) Cytokeratin-20 is a general marker of cutaneous merkel cells while certain neuronal proteins are absent. J Invest Dermat 104:910–915
Muijres FT, Johansson LC, Barfield R, Wolf M, Spedding GR, Hedenström A (2008) Leading-edge vortex improves lift in slow-flying bats. Science 319:1250–1253
Nachtigall W (1979) Gliding flight in petaurus-breviceps-papuanus. Model measurements of the influence of fur cover on flow and generation of aerodynamic force components. J Comp Physiol 133:339–349
Necker R (1985) Receptors in the wing of the pigeon and their possible role in bird flight. In: Nachtigall W (ed) Biona Rep 3: Vogelflug. Fischer, New York
Nurse CA, Mearow KM, Holmes M, Visheau B, Diamond J (1983) Merkel cell distribution in the epidermis as determined by quinacrine fluorescence. Cell Tissue Res 228:511–524
Pflueger HJ, Tautz J (1982) Air movement sensitive hairs and interneurons in locusta migratoria. J Comp Physiol A 145:369–380

Pinkus F (1902) Ueber einen bisher unbekannten nebenapparat am haarsystem des menschen: haarscheiben. Derm Z 9:465–499
Pinkus F (1905) Ueber Hautsinnesorgane neben dem menschlichen Haar (Haarscheiben) and ihre vergleichend-anatomische bedeutung. Arch Mikrosk Anat 65:121–179
Rayner JMV (1979a) Vortex theory of animal flight. 1. vortex wake of a hovering animal. J Fluid Mech 91:697–730
Rayner JMV (1979b) Vortex theory of animal flight. 2. Forward flight of birds. J Fluid Mech 91:731–763
Shimozawa T, Kanou M (1984) Variety of filiform hairs: range fractionation by sensory afferents and cercal interneurons of a cricket. J Comp Physiol A 155:485–493
Smith KR (1977) The haarscheibe. J Invest Dermat 69:68–74
Sterbing-D'Angelo S, Chadha M, Chiu C, Falk B, Xian W, Barcelo J, Zook JM, Moss CF (2011) Bat wing sensors support flight control. Proc Natl Acad Soc 108:11291–11296
Stockwell EF (2001) Morphology and flight maneuverability in new world leaf-nosed bats (chiroptera: phyllostomidae). J Zool 254:505–514
Swartz SM, Bishop K, Ismael-Aguirre MF (2005) Dynamic complexity of wing form in bats: implications for flight performance. In: Zubaid A, McCracken G, Kunz T (eds) Functional and evolutionary ecology of bats. Oxford Press, Oxford
Swartz SM, Groves MS, Kim HD, Walsh WR (1996) Mechanical properties of bat wing membrane skin. J Zool 239:357–378
Voigt CC, Winter Y (1999) Energetic cost of hovering flight in nectar-feeding bats (phyllostomidae: glossophaginae) and its scaling in moths, birds and bats. J Comp Physiol B 169:38–48
Wagner P, Neinhuis C, Barthlott W (1996) Wettability and contaminability of insect wings as a function of their surface sculptures. Acta Zool 77:213–225
Williams CM, Kramer EM (2010) The advantages of a tapered whisker. PLoS ONE 5: Article Number: e8806. doi:10.1371/journal.pone.0008806
Winter Y, Voigt C, Von Helversen O (1998) Gas exchange during hovering flight in a nectar-feeding bat, *Glossophaga soricina*. J Exp Biol 201:237–244
Wise LZ, Pettigrew JD, Calford MB (1986) Somatosensory cortical representation in the Australian ghost bat, *Macroderma gigas*. J Comp Neurol 248:257–262
Zook JM, Fowler BC (1986) A specialized mechanosensory array of the bat wing. Myotis 23–24:1–36
Zook JM (2005) The neuroethology of touch in bats: cutaneous receptors of the wing. Soc Neurosci Abstr 78:21
Zook JM (2006) Somatosensory adaptations of flying mammals, In: Kaas JH (ed) Evolution of nervous systems vol 3. Academic Press, Oxford